

Fermi surface evolution and crystal field excitations in heavy-fermion compounds probed by time-domain terahertz spectroscopy

S. Pal,¹ C. Wetli,¹ F. Zamani,² O. Stockert,³ H. v. Löhneysen,⁴ M. Fiebig,^{1,*} and J. Kroha^{2,5,†}

¹*Department of Materials, ETH Zürich, 8093 Zürich, Switzerland*

²*Physikalisches Institut and Bethe Center for Theoretical Physics, Universität Bonn, Nussallee 12, 53115 Bonn, Germany*

³*Max Planck Institute for Chemical Physics of Solids, 01187 Dresden, Germany*

⁴*Institut für Festkörperphysik and Physikalisches Institut, Karlsruhe Institute of Technology, 76021 Karlsruhe, Germany*

⁵*Center for Correlated Matter, Zhejiang University, Hangzhou, Zhejiang 310058, China*

(Dated: 16 October 2018)

We measure the quasiparticle weight in the heavy-fermion compound $\text{CeCu}_{6-x}\text{Au}_x$, ($x = 0, 0.1$) by time-resolved THz spectroscopy for temperatures from 2 K up to 300 K. This method distinguishes contributions from the heavy Kondo band and from the crystal-electric-field satellite bands by different THz response delay times. We find that the formation of heavy bands is controlled by an exponentially enhanced, high-energy Kondo scale once the crystal-electric-field states become thermally occupied. We corroborate these observations by temperature-dependent high-resolution dynamical mean-field calculations for the multi-orbital Anderson lattice model and discuss consequences for quantum critical scenarios.

In heavy-fermion materials [1], a lattice of rare-earth ions with local magnetic moments in the 4f shell is embedded in a metallic host. On lowering the temperature, the 4f electrons' magnetic moments bind to the itinerant electrons by the Kondo effect [2], thus driving part of the 4f spectral weight to the Kondo resonance near the Fermi energy ε_F . This spectral weight then forms a band of lattice-coherent, heavy quasiparticles (QPs). Consequently, part of the 4f electrons become itinerant, and the Fermi volume expands so as to accommodate the extra number of indistinguishable 4f electrons in the Fermi sea. The existence of an enlarged Fermi surface is, therefore, a unique signature of the Kondo-induced heavy Fermi-liquid phase; its absence a signature of heavy-QP destruction [3, 4], as it may occur, e.g., near a quantum phase transition (QPT) [5–7]. Within the standard Anderson lattice model, the characteristic crossover energy scale above which the Kondo correlations fade away is the Kondo lattice temperature T_K^* . However, the recent observation of a large Fermi surface in the heavy-fermion compound YbRh_2Si_2 at temperatures $T \gg T_K^*$ by angle-resolved photoemission spectroscopy (ARPES) [8] has raised disputes about the validity of this established theoretical picture [4, 8–10]. In particular, it has been questioned whether T_K^* , as extracted from low-temperature thermodynamic and transport measurements, is the correct energy scale below which the heavy QPs are formed, or whether they can persist to much higher energies [8]. This question is important, because the behavior of the QP formation scale near a heavy-fermion QPT is a hallmark distinguishing different quantum critical scenarios, like the Hertz-Moriya-Millis (spin density wave) scenario [11–13], the local quantum-critical scenario [5, 14] or other schemes of QP destruction [15–17].

In this Letter we resolve this puzzle by separately measuring the Kondo and the crystal-electric-field (CEF) contributions to the Fermi volume using time-resolved tera-

hertz (THz) spectroscopy [18] and temperature-dependent dynamical mean-field theory (DMFT) calculations. Time-domain THz spectroscopy has been recently developed as a method particularly sensitive to the QP dynamics in strongly correlated electron systems [18]. We find that for the heavy-fermion compound $\text{CeCu}_{6-x}\text{Au}_x$, the spectral weight contributing to the large Fermi surface at high temperatures is accounted for by the CEF satellite resonances of the Ce 4f orbitals, while the low-temperature behavior is controlled by the Kondo resonance, in particular near the QPT in $\text{CeCu}_{6-x}\text{Au}_x$ at $x = 0.1$. This reconciles the seemingly contradictory observation of a temperature-independent Fermi surface from the ARPES measurements [8].

CEF resonances. CEF satellite structures in heavy-fermion systems have been previously observed by photoemission [19–21] and scanning tunneling [22] spectroscopy. In order to understand their impact, one must realize that CEF resonances originate from the same strong correlation effect that generates the low-energy Kondo resonance in the first place [20, 23]. In the orthorhombic lattice structure of $\text{CeCu}_{6-x}\text{Au}_x$, the $j = 5/2$ ground-state multiplet of the Ce 4f orbitals is split by the CEF into three Kramers doublets, denoted by $\varepsilon_0, \varepsilon_1, \varepsilon_2$ (see Fig. 1). Only one of the CEF states is occupied due to strong Coulomb repulsion within the Ce 4f orbitals. By the hybridization of these orbitals with the conduction-electron states, a Ce 4f electron can fluctuate from the ground-state Kramers doublet ε_0 into a conduction state near ε_F and back to ε_0 , shown as process (0) in Fig. 1. This process involves spin exchange with the conduction electrons and is quasielastic (final and initial energies are equal, ε_0), i.e., in resonance with the low-energy conduction electron states [24, 25]. The singular quantum spin-flip scattering thus generates the narrow Kondo resonance in the Ce 4f spectrum at ε_F , shown as peak (0) in Fig. 1. Alternatively, the 4f electron can end up in one

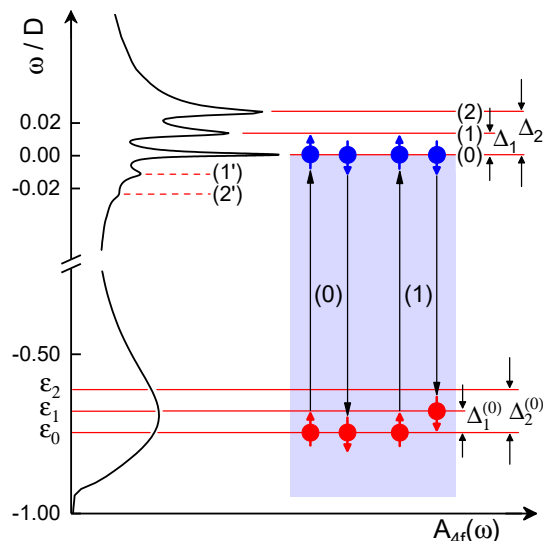


Figure 1. Ce 4f spectrum ($T \ll T_K^* < \Delta_1$) as calculated by DMFT for CeCu₆, along with a sketch of the hybridization processes generating the Kondo and CEF resonances, see text for details. The shaded region represents the occupied states of the Fermi sea. The energy scale around the Fermi energy ($\omega = 0$) is stretched by a factor 5.

of the CEF excited levels, ε_m , ($m = 1, 2$) instead of ε_0 [process (1) in Fig. 1]. Involving again singular quantum spin-flip transitions, this process generates another narrow resonance, albeit shifted in energy by the final-state excitation energy $\Delta_m = \varepsilon_m - \varepsilon_0 + \delta\Delta_m$, i.e., by the bare CEF excitation energy $\Delta_m^{(0)} = \varepsilon_m - \varepsilon_0$ and additional many-body renormalizations $\delta\Delta_m$ [peak (1) in Fig 1]. For each of the CEF satellites (1), (2) there exists a mirror satellite (1'), (2') [23] shifted downward by $-\Delta_m$, see Fig. 1. The mirror satellites appear as weak peaks or shoulders only, since they correspond to transitions from $\varepsilon_{1,2}$ to ε_0 where $\varepsilon_{1,2}$ is only virtually occupied at low temperatures. From the above discussion, it is clear that the CEF satellite resonances are of spin-scattering origin, just like the Kondo resonance itself. Thus, for $k_B T_{K,m} \lesssim k_B T \ll \Delta_1$ [see Eq. (1)] their weight has a logarithmic temperature dependence, and their width is renormalized by many-body effects to exponentially small values, analogous to the Kondo scale [2, 23],

$$T_{K,m} \approx D \exp\left(-\frac{1}{2N(0)J_m}\right), \quad (1)$$

where D is the conduction half bandwidth, $N(0)$ the (unrenormalized) density of states at the Fermi level, and J_m the effective spin exchange coupling of the conduction electrons with the CEF level $m = 0, 1, 2$, up to higher-order renormalizations [20, 23]. In fact, this narrow width makes the CEF satellite resonances energetically separated and resolvable in spectroscopic experiments [19, 20, 22] for $k_B T \ll \Delta_1$, while the hybridization width of the single-particle levels $\varepsilon_0, \varepsilon_1, \varepsilon_2$ is orders of magnitude larger than

their splitting $\Delta_m^{(0)}$, see Fig. 1. As the temperature is raised to $k_B T \approx \Delta_1$, at least one of the CEF-excited satellites becomes thermally occupied and acts as effectively degenerate levels, leading to the effective high-temperature Kondo scale

$$T_K^{(high)} \approx D \exp\left(-\frac{1}{2N(0)\sum'_m J_m}\right), \quad (2)$$

where the sum \sum'_m runs over the CEF levels m with significant thermal occupation.

To quantify this behavior, we performed DMFT calculations for the multi-orbital Anderson lattice model with three local levels ε_m , corresponding to the three Kramers doublets of the $j = 5/2$ Ce 4f ground-state multiplet in CeCu₆. The near-single occupancy of the Ce 4f shell was enforced by a strong interlevel repulsion, $U \rightarrow \infty$. The multi-orbital non-crossing approximation (NCA) [20] has been used as the DMFT impurity solver. For a single Anderson impurity in the $U \rightarrow \infty$ limit, the NCA is known to correctly describe the width and temperature dependence of the spectral features mentioned above from high T down to well below T_K^* [20, 26]. We chose the bare model parameters such that the DMFT calculations produce the values for T_K^* and the CEF splittings reported in the literature [21, 27–29], see below. The resulting DMFT spectra $A_{4f}(\omega)$ in Fig. 3(a) exhibit the crossover from the high-temperature scale $T_K^{(high)} \approx 200 \text{ K} \hat{=} 17 \text{ meV}$ to the low-energy Kondo scale $T_K^* = T_{K,0} \approx 6 \text{ K} \hat{=} 0.52 \text{ meV}$.

Time-resolved THz spectroscopy. We investigate the temperature dependence of the QP spectral weight in the CeCu_{6-x}Au_x system. CeCu₆ has a Kondo lattice scale of $T_K^* \approx 6 \text{ K}$ and CEF excitations at $\Delta_1 = 7 \text{ meV}$ and $\Delta_2 = 13 \text{ meV}$ [27–29]. CeCu_{6-x}Au_x undergoes a magnetic QPT at $x = 0.1$ [1]. We generate THz pulses of 1.5 cycles duration, covering a frequency range of 0 - 3 THz, by optical rectification in a 0.5 mm (110)-oriented ZnTe crystal and radiate these pulses onto samples of the Fermi-liquid compound CeCu₆ and of the quantum-critical compound CeCu_{5.9}Au_{0.1}. The reflected THz electric field is detected via free-space electrooptic sampling on a 0.5 mm (110)-oriented ZnTe crystal that is optically bonded to a 2 mm (100)-oriented ZnTe crystal, using lock-in techniques. In this way, time traces of the reflected signal are taken from $t = -4 \text{ ps}$ to $+8.5 \text{ ps}$ in steps of 0.04 ps. All time traces are normalized by a factor such that the integrated intensity equals one, representing identical total reflected power. It has been shown previously [18] that a correlated many-body state manifests itself in the reflected THz electric field as a temporally confined and delayed pulse whose delay time resembles the QP lifetime (inverse spectral width), its integrated weight the QP weight. In particular, for a band of heavy Kondo QPs with spectral width $k_B T_K^*$ the delay time is $\tau_K^* = h/k_B T_K^*$, with h the Planck constant and k_B the Boltzmann constant [18]. The temporally delayed pulse thus provides a direct and background-free probe for the QP dynamics of strongly correlated states.

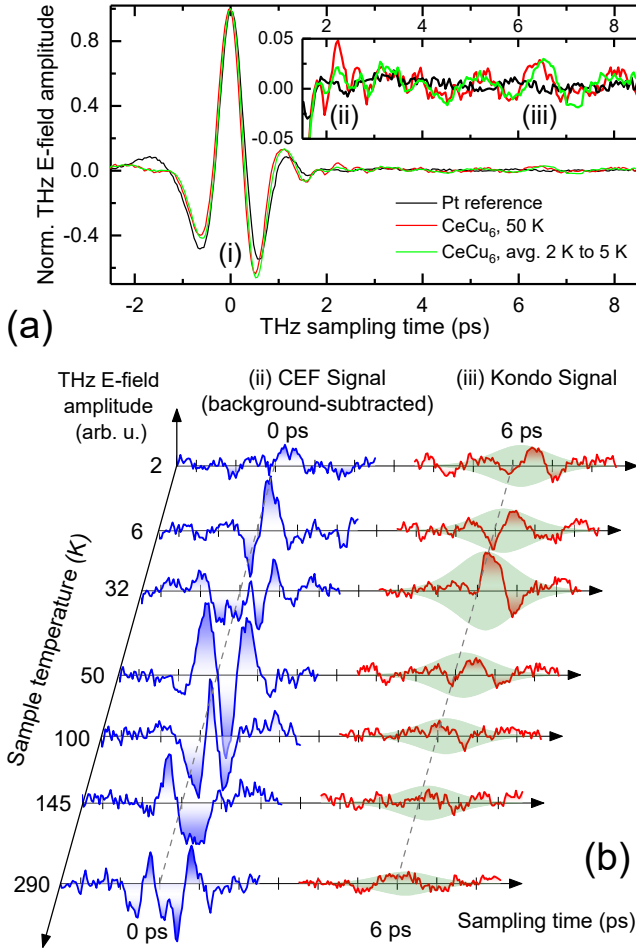


Figure 2. (a) Time traces of the THz electric field reflected from a CeCu_6 sample at $T = 50$ K (red) in comparison to a Pt reference at $T = 2.0$ K (black) and the average of the CeCu_6 time traces for temperatures between 2.0 and 5.0 K (green). (b) Evolution of the background-subtracted CEF signal (-2.5 ps to $+2.5$ ps) and the Kondo signal ($+3.5$ ps to $+8.5$ ps) as the temperature of the heavy-fermion sample decreases from room temperature down to 2 K. The green-shaded region depicting the envelope of the Kondo signal is a solution of the non-linear rate equation of Ref. [18] describing the relaxation of the THz-excited heavy-fermion system with a single local orbital. Trivial delayed reflexes originating from the THz generation crystal or the cryostat windows have been identified at times $t > 10$ ps, outside the considered time window [18].

Analysis of spectral features. A THz signal reflected from a CeCu_6 sample is shown in Fig. 2 (a) in comparison to a platinum reference signal. It exhibits three distinct features labeled (i), (ii), (iii). In the time interval $[-2.5$ ps, $+2.5$ ps] the signal consists of two overlapping features (i) and (ii). The strong, instantaneous pulse (i) centered at $t = 0$ ps appears almost identically in CeCu_6 and in Pt and is temperature independent [not shown in Fig. 2 (a)]. It is the stimulated single-particle response of the light conduction electrons. In addition, there is a weaker feature (ii) visible as the wiggles superimposed on the wing of pulse (i). We

observe that this signal does not appear in the Pt reference, has a reproducible, nonmonotonic temperature dependence (analyzed below), and vanishes in all measured time traces below $T = 5$ K. We use this temperature dependence to separate signal (ii) from the single-particle reflex (i): We take the temperature average of the time traces taken between 2 K and 5 K and subtract it from each time trace within the time interval $[-2.5$ ps, $+2.5$ ps]. Finally, the pulse (iii), centered around 6 ps, has been identified earlier [18] with the Kondo resonance by its characteristic temperature dependence [c.f. Fig. 2(b)] and by its delay time agreeing well with the Kondo QP lifetime τ_K^* . For the detailed analysis of this signal see Ref. [18].

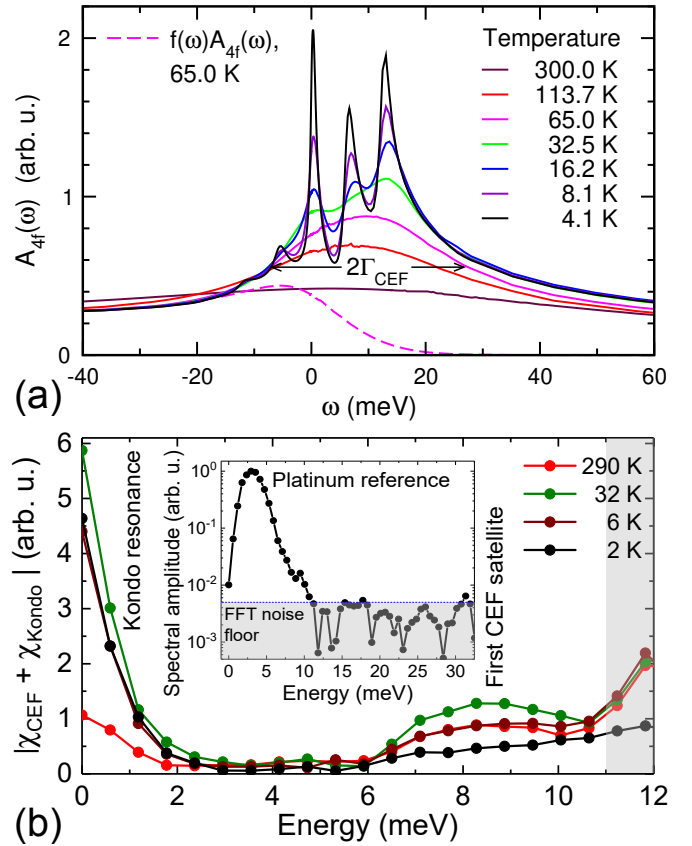


Figure 3. (a) Temperature dependence of the momentum-integrated Ce 4f spectral density in CeCu_6 (solid lines), as calculated by DMFT for the Anderson lattice model. The occupied spectral density at 65.0 K, $f(\omega)A_{4f}(\omega)$ (dashed line; $f(\omega)$ is the Fermi-Dirac distribution), visualizes that the spectral width, $\Gamma_{\text{CEF}} = k_B T_K^{(\text{high})} \approx 17$ meV $\hat{=} 200$ K, is not accounted for by thermal broadening at 65.0 K alone. (b) Magnitude spectrum of the CEF and Kondo responses of CeCu_6 . The Kondo response peaks near zero energy, and has a width of 0.56 meV ($\hat{=} 6.7$ K) which agrees very well with $k_B T_K^*$. The CEF response shows the first CEF satellite at 8 meV, close to the literature value [27–29]. The gray-shaded region is beyond the spectral width of the THz excitation, i.e., governed by noise. The Pt reference, equivalent to the incident THz spectrum $|E_{\text{in}}(\omega)|$, is shown in the inset.

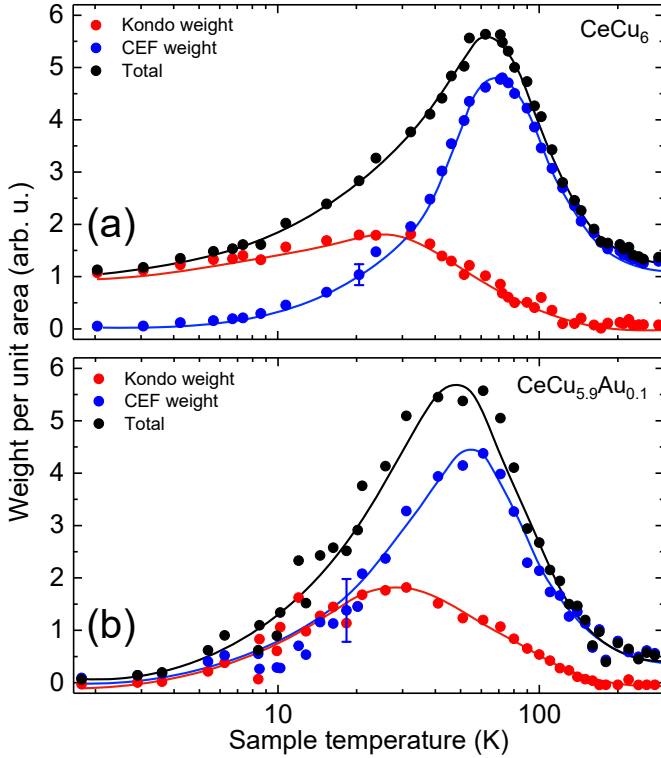


Figure 4. Temperature dependence of the occupied weights of the Kondo (red) and of the CEF (blue) bands as well as the sum of the two (black) for (a) CeCu_6 and (b) $\text{CeCu}_{5.9}\text{Au}_{0.1}$. The error bars shown result from averaging over 10 measurements for each data point taken within a time trace.

The resulting, correlation-induced and background-subtracted time traces are shown in Fig. 2(b). The amplitude of the signal (iii) from the heavy Kondo band rises with decreasing temperature and remains finite at the lowest temperatures, with some decrease due to the vicinity of the QPT [18]. The background subtraction reveals that the reflex (ii) is not only located around 2 ps, but extends over a wider time range centered around the short delay time of $\tau_{\text{CEF}} \approx 0.25$ ps. It also rises with decreasing temperature, but reaches a maximum near $T = 60$ K and then decreases to undetectably small values for $T \lesssim 5$ K. Such nonmonotonic behavior is a clear signature of the CEF resonances, as can be seen from the DMFT calculations of Fig. 3(a): On reducing the temperature, a single, broad resonance of width $\Gamma_{\text{CEF}} = k_B T_K^{(\text{high})} \approx 17$ meV rises up, corresponding to the increase of the signal (ii) in Fig. 2(b). Below about 60 K the broad resonance in Fig. 3(a) splits into three individual, sharp CEF peaks of which only the lowest one is occupied towards $T = 0$. Correspondingly, the short-delayed signal (ii) in Fig. 2(b) disappears, and part of its weight reappears in the Kondo pulse (iii) with $\tau_K^* = h/k_B T_{K,0} = h/k_B T_K^* = 6$ ps delay time. Hence, we have unambiguously associated the time traces (ii) in Fig. 2(b) to the broad CEF resonance of Fig. 3(a).

Further evidence for the CEF satellites is provided from

the spectral analysis using the (non-equilibrium) response function $\chi(\omega) = E_{\text{out}}(\omega)/E_{\text{in}}(\omega)$ which we define as the ratio of the Fourier transforms of the reflected signal from the sample, $E_{\text{out}}(\omega)$, and the incident light pulse $E_{\text{in}}(\omega)$ (given by the Pt reference in the present case). The magnitude spectrum of the sum of the response functions $\chi_{\text{CEF}}(\omega)$ and $\chi_{\text{Kondo}}(\omega)$ resulting from the traces (ii) and (iii) of Fig. 2(b), respectively, is shown in Fig. 3(b). It clearly exhibits the Kondo resonance and the first CEF satellite resonance, including their characteristic temperature dependences.

Large Fermi volume at high temperatures. We are now in a position to analyze separately the Fermi volume change induced by the low-temperature Kondo effect and by the CEF excitations. We integrate, after background subtraction, the time traces of the squared THz electric field over the time intervals $[-2.5 \text{ ps}, +2.5 \text{ ps}]$ (ii) and $[+3.5 \text{ ps}, +8.5 \text{ ps}]$ (iii) in Fig. 2(b). The weights calculated in this way represent directly the total occupation numbers of the heavy Kondo and CEF satellite bands near ε_F , respectively, since the THz excitation is, of course, sensitive to occupied states only. Thus, these weights directly account for the correlation-induced Fermi volume change. The temperature-dependent results are shown for CeCu_6 in Fig. 4(a). The Kondo as well as the CEF weights rise log-

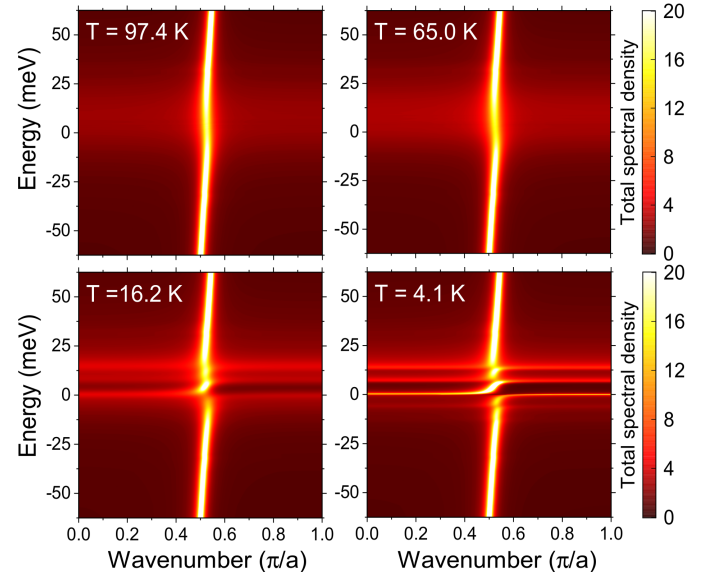


Figure 5. Band structure near the Fermi energy as calculated by DMFT for a three-orbital Anderson lattice for a sequence of temperatures. The model parameter values are chosen in order to resemble CeCu_6 , $T_K^* \approx 6$ K and $\Delta_1 = 7$ meV, $\Delta_2 = 13$ meV. The nearly vertical line represents the light conduction band. At low temperatures, $T \lesssim T_K^*$, the sharp, heavy Ce 4f Kondo and CEF satellite bands are well resolved, each one hybridizing with the conduction band. At high temperatures, $T \gtrsim \Delta_1$, they merge to a single, heavy band of shorter lifetime, which still has significant spectral weight at the Fermi energy, thus maintaining a large Fermi volume up to $T \gtrsim T_K^{(\text{high})} \gg T_K^*$.

arithmically with decreasing temperature, once again confirming that both are of Kondo-like origin. The Kondo weight reaches a maximum near $T = 30$ K and settles to a finite value at the lowest temperatures. The CEF weight dominates the high-temperature behavior, with a characteristic temperature of $T_K^{(high)} \approx 200$ K $\hat{=}$ 17 meV, read off from the onset of its logarithmic rise and in good quantitative agreement with the CEF resonance width at high temperature obtained from DMFT [Fig. 3(a)]. The CEF weight vanishes gradually below ~ 60 K, when the CEF satellite occupation gets frozen out and is transferred to the rising Kondo weight. This complex behavior is confirmed by the momentum-resolved DMFT calculations, shown in Fig. 5. Thus, our experimental findings and theoretical calculations reveal consistently that an enlarged Fermi volume persists at temperatures much higher than T_K^* due to the CEF satellite contributions, but it is carried by the Kondo spectral weight alone when the temperature is lowered below the CEF splitting Δ_1 . The results of analogous measurements for the quantum critical compound $\text{CeCu}_{5.9}\text{Au}_{0.1}$ are shown in Fig. 4(b). We see that the CEF contribution to the Fermi volume is almost identical to that in the Fermi-liquid compound CeCu_6 for all temperatures. However, the Kondo spectral weight is seen to vanish at the quantum critical point in $\text{CeCu}_{6-x}\text{Au}_x$.

Conclusion. Time-domain THz spectroscopy provides a nearly background-free probe of quasiparticle dynamics in correlated electron systems with a characteristic energy scale in the THz range. Our measurements on $\text{CeCu}_{6-x}\text{Au}_x$ along with the DMFT calculations show that the spectral weight near the Fermi level is governed by a heavy-quasiparticle state whose width crosses over from the CEF-induced high-energy scale $T_K^{(high)}$ to the Kondo lattice scale T_K^* at low temperature. THz reflection acts as a "time filter" separating the CEF excitations from the Kondo resonance by a different reflex delay time. Thanks to this, we showed that at high temperatures of $T \approx T_K^{(high)} \gg T_K^*$ the Fermi volume is enlarged by the CEF excitations, both in the Fermi liquid phase (CeCu_6) and in the quantum critical compound $\text{CeCu}_{5.9}\text{Au}_{0.1}$. At low temperatures $T < \Delta_1$, the large Fermi volume is carried by the ground-state Kondo band in CeCu_6 , but collapses at the QPT [18]. This reconciles, within a single experiment, the existence of a large Fermi volume at $T \gg T_K^*$ with Kondo destruction at the QPT.

The authors gratefully acknowledge insightful discussions with S. Kirchner, K. Kliemt, C. Krellner, K. Matho, S. Wirth, and G. Zwirgagl. This work was financially supported by the Swiss National Science Foundation (SNSF) via projects No. 200021_147080 (M.F., C.W.) and 200021_178825 (M.F., S.P.) and by the Deutsche Forschungsgemeinschaft (DFG) via grant No. SFB/TR 185-C4 (J.K., F.Z.).

* manfred.fiebig@mat.ethz.ch

† kroha@physik.uni-bonn.de

- [1] H. v. Löhneysen, A. Rosch, M. Vojta, and P. Wölfle, *Fermi-liquid instabilities at magnetic quantum phase transitions*, Rev. Mod. Phys. **79**, 1015 (2007).
- [2] A. C. Hewson, *The Kondo problem to heavy fermions* (Cambridge University Press, Cambridge, England, 1993).
- [3] A. Benlagra, T. Pruschke, and M. Vojta, *Finite-temperature spectra and quasiparticle interference in Kondo lattices: From light electrons to coherent heavy quasiparticles*, Phys. Rev. B **84**, 195141 (2011).
- [4] H. C. Choi, B. I. Min, J. H. Shim, K. Haule, and G. Kotliar, *Temperature-dependent Fermi surface evolution in heavy fermion CeIrIn_5* , Phys. Rev. Lett. **108**, 016402 (2012).
- [5] P. Coleman, C. Pépin, Q. Si, and R. Ramazashvili, *How do Fermi liquids get heavy and die?*, J. Phys. Condens. Matter **13**, R723 (2001).
- [6] A. Hackl and M. Vojta, *Kondo volume collapse, Kondo breakdown, and Fermi surface transitions in heavy-fermion metals*, Phys. Rev. B **77**, 134439 (2008).
- [7] S. Friedemann, N. Oelscher, S. Wirth, C. Krellner, C. Geibel, F. Steglich, S. Paschen, S. Kirchner, Q. Si, *Fermi surface collapse and dynamical scaling near a quantum critical point*, PNAS **107**, 14547 (2010).
- [8] K. Kummer, S. Patil, A. Chikina, M. Güttler, M. Höppner, A. Generalov, S. Danzenbächer, S. Seiro, A. Hannaske, C. Krellner, Yu. Kucherenko, M. Shi, M. Radovic, E. Rienks, G. Zwirgagl, K. Matho, J. W. Allen, C. Laubschat, C. Geibel, and D. V. Vyalikh, *Temperature-independent Fermi surface in the Kondo lattice YbRh_2Si_2* , Phys. Rev. X **5**, 011028 (2015).
- [9] S. Paschen, S. Friedemann, S. Wirth, F. Steglich, S. Kirchner, and Q. Si, *Kondo destruction in heavy fermion quantum criticality and the photoemission spectrum of YbRh_2Si_2* , J. Mag. Mag. Mat. **400**, 17 (2016).
- [10] Q. Y. Chen, D. F. Xu, X. H. Niu, J. Jiang, R. Peng, H. C. Xu, C. H. P. Wen, Z. F. Ding, K. Huang, L. Shu, Y. J. Zhang, H. Lee, V. N. Strocov, M. Shi, F. Bisti, T. Schmitt, Y. B. Huang, P. Dudin, X. C. Lai, S. Kirchner, H. Q. Yuan, and D. L. Feng, *Direct observation of how the heavy-fermion state develops in CeCoIn_5* , Phys. Rev. B **96**, 045107 (2017).
- [11] J. A. Hertz, *Quantum critical phenomena*, Phys. Rev. B **14**, 1165 (1976).
- [12] T. Moriya, *Spin fluctuations in itinerant electron magnetism*, (Springer, Berlin, 1985).
- [13] A. Millis, *Effect of a nonzero temperature on quantum critical points in itinerant fermion systems*, Phys. Rev. B **48**, 7183 (1993).
- [14] Q. Si, S. Rabello, K. Ingersent and J. L. Smith, *Locally critical quantum phase transitions in strongly correlated metals*, Nature (London) **413**, 804 (2001).
- [15] T. Senthil, M. Vojta and S. Sachdev, *Weak magnetism and non-Fermi liquids near heavy-fermion critical points*, Phys. Rev. B **69**, 035111 (2004).
- [16] P. Wölfle and E. Abrahams, *Quasiparticles beyond the Fermi liquid and heavy fermion criticality*, Phys. Rev. B **84**, 041101(R) (2011).
- [17] A. Nejadi, K. Ballmann, and J. Kroha, *Kondo destruction in RKKY-coupled Kondo lattice and multi-impurity systems*, Phys. Rev. Lett. **118**, 117204 (2017).
- [18] C. Wetli, S. Pal, J. Kroha, K. Kliemt, C. Krellner, O. Stockert, H. v. Löhneysen, and M. Fiebig, *Time-resolved col-*

- lapse and revival of the Kondo state near a quantum phase transition*, Nature Phys., DOI: 10.1038/s41567-018-0228-3 (2018).
- [19] F. Reinert, D. Ehm, S. Schmidt, G. Nicolay, and S. Hüfner, J. Kroha, O. Trovarelli and C. Geibel, *Temperature dependence of the Kondo resonance and its satellites in CeCu₂Si₂*, Phys. Rev. Lett. **87**, 106401 (2001).
- [20] D. Ehm, S. Schmidt, S. Hüfner, F. Reinert, J. Kroha, P. Wölfle, O. Stockert, C. Geibel and H. von Löhneysen, *High resolution photoemission study on low- T_K Ce systems: Kondo resonance, crystal field structures, and their temperature dependence*, Phys. Rev. B **76**, 045117 (2007).
- [21] M. Klein, A. Nuber, F. Reinert, J. Kroha, O. Stockert, and H. v. Löhneysen, *Signature of quantum criticality in photoemission spectroscopy at elevated temperature*, Phys. Rev Lett. **101**, 266404 (2008).
- [22] S. Ernst, S. Kirchner, C. Krellner, C. Geibel, G. Zwicknagl, F. Steglich, and S. Wirth, *Emerging local Kondo screening and spatial coherence in the heavy-fermion metal YbRh₂Si₂*, Nature **474**, 362 (2011).
- [23] J. Kroha, S. Kirchner, G. Sellier, P. Wölfle, D. Ehm, F. Reinert, S. Hüfner, and C. Geibel, *Structure and transport in multi-orbital Kondo systems*, Physica E **18**, 69 (2003).
- [24] J. R. Schrieffer and P. A. Wolff, *Relation between the Anderson and Kondo Hamiltonians* Phys. Rev. **149**, 491 (1966).
- [25] F. Zamani, P. Ribeiro, and S. Kirchner, *The functional integral formulation of the Schrieffer-Wolff transformation*, New J. Phys. **18**, 063024 (2016).
- [26] T. A. Costi, J. Kroha, and P. Wölfle, *Spectral properties of the Anderson impurity model: comparison of numerical renormalization group and non-crossing approximation*, Phys. Rev. B **53**, 1850 (1996).
- [27] B. Stroka, A. Schröder, T. Trappmann, H. v. Löhneysen, M. Loewenhaupt, and A. Severing, *Crystal-field excitations in the heavy-fermion alloys CeCu_{6-x}Au_x studied by specific heat and inelastic neutron scattering*, Z. Phys. B **90**, 155 (1993).
- [28] E. A. Goremychkin and R. Osborn, *Neutron-spectroscopy study of the heavy-fermion compound CeCu₆*, Phys. Rev. B **47**, 14580 (1993).
- [29] U. Witte, R. Schedler, O. Stockert, and M. Loewenhaupt, *The Investigation of the Crystalline Electric Field of CeCu₂ and CeCu₆*, J. Low Temp. Phys. **147**, 97 (2007).
- [30] S. Doniach, *Kondo lattice and weak antiferromagnetism*, Physica B+C **91**, 231 (1977).